*Int. J. Electrochem. Sci.*, 8 **(2013)** 7345 - 7356

International Journal of
ELECTROCHEMICAL
SCIENCE
www.electrochemsci.org

# Direct Electron Transfer of Myoglobin on CdO Nanoparticles Modified Glassy Carbon Electrode

*Nooshin Mohammadi*[1], *Yousoof Ghanbari-kakavandi*[2], *Ali Akbar Movassagh*[3], *Somayeh Nasereslami*[4], *Gholamreza Mohseni*[5], *Abbas Hajiosseinlo*[6], *Leila Sofimaryo*[2], *Reza Soleimani*[2], *Hajar Akbari-dastjerdi*[2], *Masoud Negahdary*[7,*]

[1] Department of Anesthetics, Shahid Beheshti University of Medical Sciences, Tehran, Iran
[2] Department of Biology, Payame Noor University, I.R. of IRAN
[3] Department of Electrical Engineering, Sharif University of Technology, Tehran, Iran
[4] Department of Biology, Science and Research Branch, Islamic Azad University, Tehran, Iran
[5] Department of Anesthetics, Shahid Beheshti University of Medical Sciences, Tehran, Iran
[6] Department of Animal Science, Faculty of Agriculture, University of Urmia, Iran
[7]Young Researchers and Elites Club, Marvdasht Branch, Islamic Azad University, Marvdasht, Iran
[*]E-mail: Masoud.negahdary@hotmail.com

*Received:* 16 December 2012 / *Accepted:* 28 January 2013 / *Published:* 1 May 2013

In this study, direct electron transfer of myoglobin (Mb) on cadmium oxide (CdO) nanoparticles modified glassy carbon electrode (GCE) was investigated. Prepared CdO nanoparticles were studied by X-Ray diffraction (XRD) and UV–visible absorption methods. All electrochemical studies were performed by cyclic voltammetry (CV) and a potentiostat device. The cyclic voltammogram of Mb/ CdO Nps/ GCE showed a couple of stable redox and oxidative peaks at -470 and -370 mV at scan rate of 50 $mVs^{-1}$, respectively. The formal potential ($E^o$) of myoglobin was calculated as -(420 ± 3) mV. Direct electrode transfer led to design a biosensor for determination of hydrogen peroxide ($H_2O_2$). The sensor sensitivity was found in the range of 50 to 1150 µM of $H_2O_2$. Designed biosensor showed a good reproducibility and stability.

**Keywords:** Bioelectrochemistry, Myoglobin, Cadmium oxide (CdO) nanoparticles, Glassy Carbon Electrode

## 1. INTRODUCTION

Electrochemistry involves chemical phenomena associated with charge separation, which often results in charge transfer. Charge transfer can occur homogeneously in solution, or heterogeneously on electrode surfaces [1]. The investigation of direct electron transfer between redox proteins and electrodes is of great importance in the development of electroanalytical applications and

bioelectrocatalytic devices [2-5]. Electron transfer reactions of metalloproteins at functional electrodes are subjects of interest in bioelectrochemistry and related fields [6]. Recently, in many electrochemical processes, nanotechnology is employed to speed and facilitate electron transfer [7-9]. Nanotechnology, the understanding and control of matter at dimensions of roughly one to one hundred billionths of a meter, has created a revolution in science and industry worldwide [10-11]. Nanotechnology and Nanoscience deal with structures at a scale smaller than 100 nm ($1nm=10^{-9}m$). The reduced size of nanomaterials leads to considerably different properties including exceptional mechanical, optical, magnetic and electrical properties compared to bulk materials [12]. As a consequence, these fields have attracted considerable interest in the last decade [13-14]. The basic interest in nanotechnology was initially limited to research labs mainly of physics and chemistry and more lately to that of materials science. However, daily applications are increasing as well as the fields of applications [16]. Semiconductor nanoparticles that exhibit quantum confinement are an important component in many emerging nanotechnologies, and will become part of our lives in years to come. Cadmium oxide (CdO) is II-VI n-type semiconductor used as an electron transfer facilitator in electrochemical sections in this study. The cdo nanoparticles is insoluble in water and also has large band gap (2.5 eV direct band gap9 and 1.98 eV indirect band gap), low electrical resistivity and high transmission in the visible region etc; which makes it useful for a wide range of applications such as biosensors and electrochemical devices. Various nanotechnology-based devices such as biosensors have been designed which involve in the detection of hydrogen peroxide ($H_2O_2$), pesticides, herbicides, insecticide, viruses, microbe [17-18]. Myoglobin (Mb) is one of the most important proteins in the human body found in muscle tissue, at which it binds oxygen, helping to provide extra oxygen to release energy to power muscular contractions [19-20]. As a heme-containing protein myoglobin involves in the transport and short-term storage of oxygen [21]. Much research has been focused on the study of the electron-transfer reaction of Mb on electrodes [22-24]. Myoglobin is a water-soluble globular protein of ~ 150 amino acids. The tertiary structure is composed of eight α-helices joined by short non-helical regions [25]. The helices provide a rigid structural framework for the heme pocket. A heme group, located in a hydrophobic cleft in the protein, is a key to the function of myoglobin: it is to the heme that oxygen binds [26]. The molecular structure of Mb was shown in figure 1.

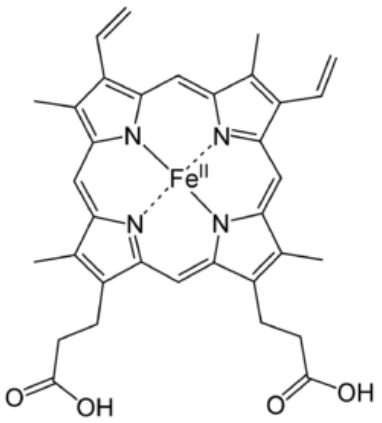


**Figure 1.** Molecular structure of myoglobin

Cadmium oxide (CdO) attracts tremendous attention due to its interesting properties particularly direct band gap of 2.5 ev [27-28]. In the present paper, synthesis and the characterization of cadmium oxide nanoparticles were performed [29]. Furthermore, glassy carbon electrode, the most common form of carbon electrode, was modified–with cadmium oxide nanoparticles and used as working electrode.

## 2. EXPERIMENTAL

### *2.1. Materials*

Myoglobin, cadmium acetate and ammonia solution were purchased from Sigma-Aldrich. Other Reagents were obtained from Merck. Supporting electrolyte used for all experiments was phosphate buffer solution (PBS) (0.1 M, pH 7). Aqueous solutions were prepared using double distilled water generated by a Barnstead water system. All reagents used were of analytical grade.

### *2.2. Apparatus*

Cyclic voltammetry (CV) and square wave voltammetry were performed using an Autolab potentiostat PGSTAT 302 (Eco Chemie, Utrecht, The Netherlands) driven by the General purpose Electrochemical systems data processing software (GPES, software version 4.9, Eco Chemie). A conventional three-electrode cell comprising a bare or CdO nanoparticles modified glassy carbon electrode (3.0mm diameter) as a working electrode, a saturated calomel electrode (SCE) as a reference electrode, and a platinum electrode as a counter electrode was employed throughout the experiments. The phase characterization of CdO nanoparticles was performed by means of X-ray diffraction (XRD) using a D/Max-RA diffractometer with CuK$\alpha$ radiation. The absorbance properties of prepared nanoparticles were measured and recorded by using a TU-1901 double-beam UV-visible spectrophotometer. The morphologies and particle sizes of the samples were characterized by scanning electron microscopy (SEM) using ZIESS EM 902A scanning electron microscope.

### *2.3. Synthesis of CdO nanoparticles*

To produce cadmium oxide nanoparticles, cadmium acetate (6.66 g, 0.5 M) was dissolved in 100 ml water and the pH of solution was adjusted to 8 with ammonia solution. The white precipitate was allowed to settle for 5-6 hours and then filtered and washed 3-4 times with water. It was dried at 100°C and then grinded. The resulting powder was calcined at 400°C for 2 hours. It turned into yellowish colour which confirmed the formation of CdO. The following equation shows the schematic diagram for the preparation of CdO nanoparticles.

$$(CH_3COO)_2\,Cd{\cdot}H_2O + 2NH_4OH \rightarrow Cd\,(OH)_2 + 2H_2O + 2CH_3COONH_4$$

During calcination at 400 °C, the prepared powder loses $H_2O$ as follows:

$$Cd(OH)_2 \rightarrow CdO + H_2O$$

*2.4. Preparation of unmodified glassy carbon electrode*

Glassy carbon (GC) is the most commonly used carbon-based electrode widely used in the analytical laboratory. It is made by pyrolyzing (Pyrolysis is the thermal decomposition of organic compounds to high temperatures in the absence of oxygen) a carbon polymer to a high temperature (e.g. 2000°C) under carefully controlled conditions [29]. An intertwining ribbon-like material results with retention of high conductivity, hardness, and inertness. Glassy carbon electrode (dia. 3mm) was polished with 1 $\mu$m and 0.05 $\mu$m alumina slurries sequentially and then washed with distilled water. Afterward, the electrode was sonicated in deionized water and finally dried under ambient conditions.

*2.4. Preparation of modified glassy carbon electrode with CdO nanoparticles and Mb*

To prepare the modified GCE with CdO nanoparticles and Mb, CdO nanoparticles were firstly immobilized on GCE surface, the CdO nanoparticles /glassy carbon electrode was placed into a fresh PBS including 10mg $mL^{-1}$ Mb (pH 7.0, 3 to 5°C) for 8 hours. Finally, the modified electrode was washed with deionized water and stored in PBS (PH 7.0) at 4°C being employed as working electrode.

## 3. RESULTS AND DISCUSSION

*3.1. X-Ray diffraction of CdO nanoparticles*

The XRD pattern of CdO nanoparticles is shown in Fig. 2 , the diffraction peaks are absorbed at 2θ values. The prominent peaks have been utilized to estimate the grain size of sample according to Scherrer equation [30]:

$$D = K\lambda/(\beta \cos \theta)$$

where K is a geometric factor (K= 0.9), λ is the wavelength (λ = 1.5418 A°) (Cu Kα), β is the full width at the half-maximum of the line and θ is the diffraction angle. The grain size was estimated using the relative intensity peak of CdO nanoparticles which was found to be 30 nm. The increase in sharpness of XRD peaks indicates the crystalline nature of CdO nanoparticles. The reflections are clearly observed which closely match to the reference patterns of CdO (Joint Committee for Powder Diffraction Studies (JCPDS) File No. 05-0640).

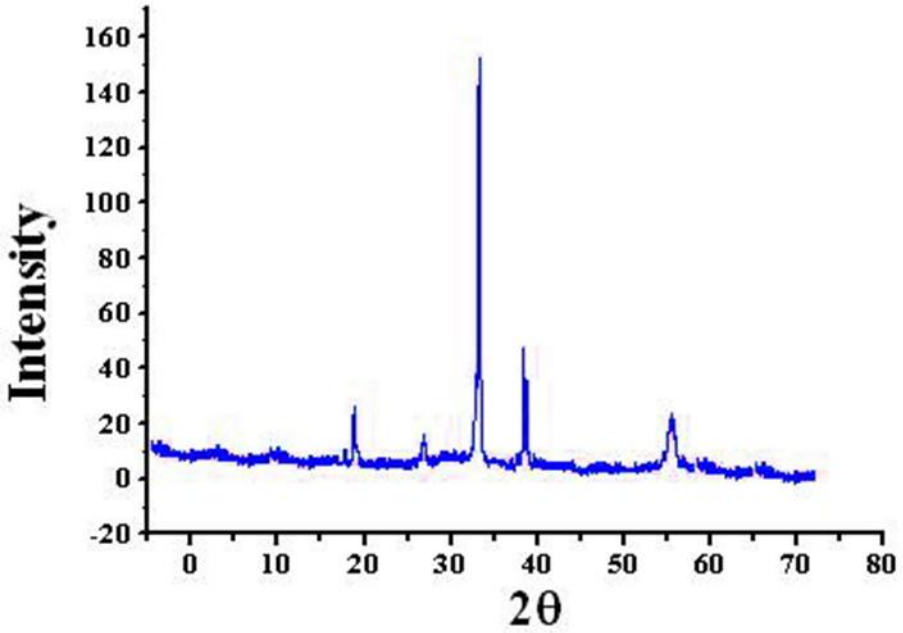


**Figure 2.** XRD pattern for CdO nanoparticles

*3.2. UV–visible absorption spectra of CdO nanoparticles*

The UV–visible absorption spectra of CdO nanoparticles are shown in Fig. 3. The absorption band of the CdO nanoparticles exhibits a blue shift due to the quantum confinement in sample compared to bulk CdO particles. This optical phenomenon indicated that these nanoparticles showed the quantum size effect [31].

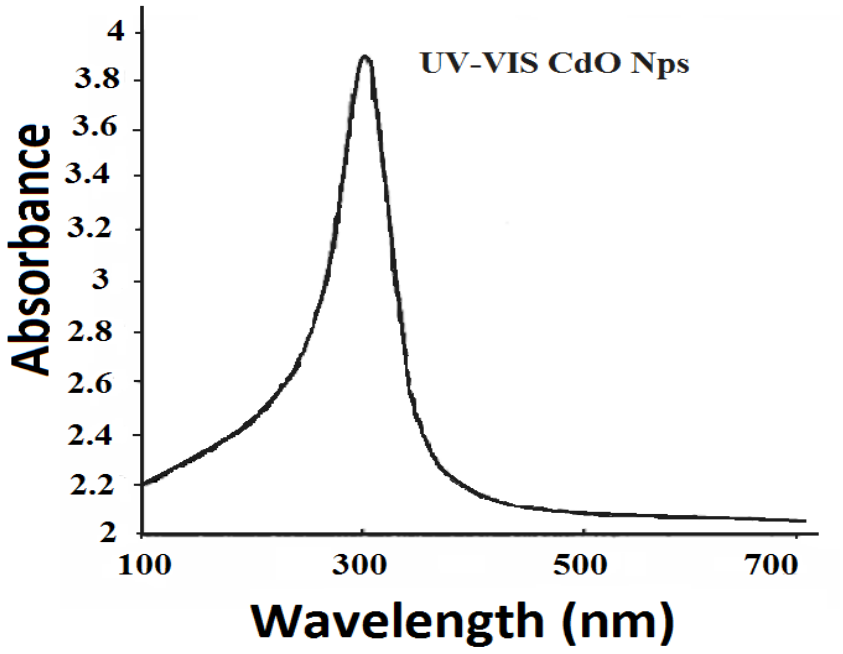


**Figure 3.** UV-Absorption spectra for CdO nanoparticles

*3.3. Microscopic characterization of CdO nanoparticles*

Scanning electron microscopy (SEM) was employed to analyze the nano-scale distribution of CdO nanoparticls (Fig. 4a and b).

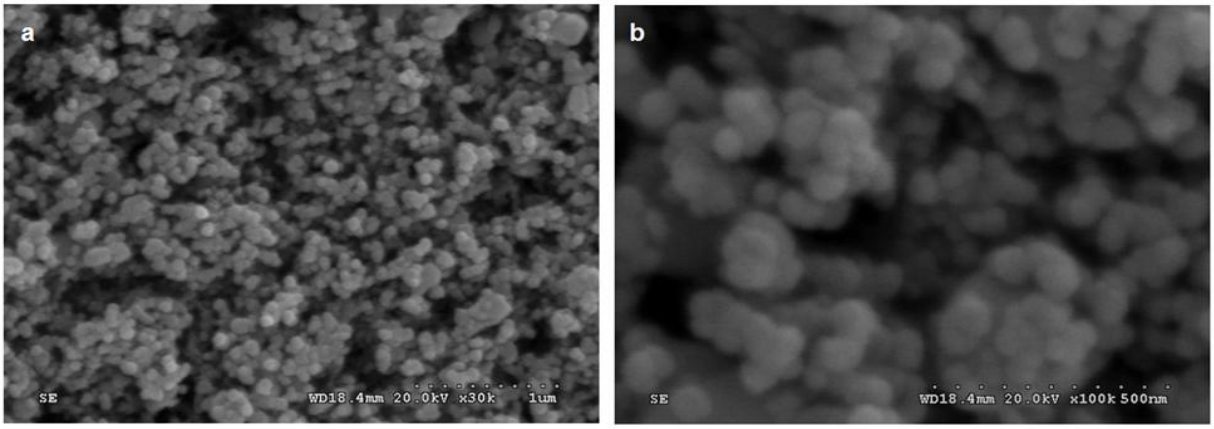


**Figure 4.** Microscopic characterization of CdO nanoparticles

As the size of nanoparticles decreased, the ratio of surface-to-volume increased. This feature represents the significant role of nanoparticles in immobilization processes. Based on SEM results, the synthesized CdO nanoparticles averaged in 25-30 nm. The scale bars in Fig. 4a and b represent 1 μm and 500 nm, respectively.

*3.4. Direct electrochemistry of the modified glassy carbon electrode with Mb and CdO nanoparticles*

Fig. 5 illustrates the cyclic voltammograms (CV) of bare GCE and Mb/ CdO Nps/ GCE in 0.1M PBS, pH 7.0. No obvious electrochemical response was observed for bare GCE (fig. 5a). In contrast, the cyclic voltammogram of Mb/ CdO Nps/ GCE exhibited a couple of stable redox and oxidative peaks at -470 and -370 mV at scan rate of $50mVs^{-1}$ respectively (Fig. 5b). CdO nanoparticles could facilitate fast direct electron transfer between redox proteins and electrode surface. Obviously, these peaks were attributed to the redox reaction of the electroactive heme center of myoglobin. Mb/GCE also showed a response (not shown here) to conventional three-electrode cell, but much smaller than that of Mb/ CdO Nps/ GCE. Thus, the adsorption of myoglobin and cadmium oxide nanoparticles on the electrode surface played a crucial role in facilitating the electron exchange between the electroactive heme center of myoglobin and GCE. The formal potential ($E^o$) of myoglobin, estimated as the midpoint of reduction and oxidation potentials, was calculated as -(420 ± 3) mV (Fig. 5a and b).

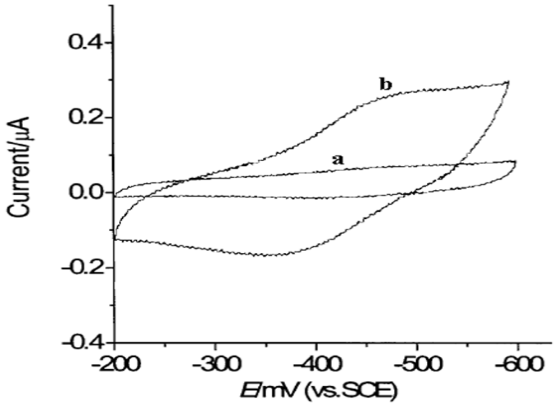


**Figure 5.** Cyclic voltammograms of (a) bare GCE and (b) Mb/ CdO Nps/ GCE in (0.1 M PBS and scan rate. 50 mV/s).

The collected voltammograms in Fig. 6a substantiates a statement that the nanometer-scale of cadmium oxide nanoparticles could play a key role in the creation of the myoglobin CV response. Scientifically, the surface-to-volume ratio increases with decreasing nanoparticle size and the protein size is comparable with the nanometer-scale building blocks, therefore nanoparticles displayed a great effect on the electron exchange between myoglobin and glassy carbon electrode. For further investigation on the myoglobin characteristics at the Mb/ CdO Nps/ GCE electrode, the effect of different scan rates (50, 100, 200, 300, 400 and 500 mv/s) on the myoglobin voltammetric behavior was studied in detail. The baseline subtraction procedure for the cyclic voltammograms was obtained in accordance with the method reported by Bard and Faulkner [32]. The scan rate (ν) and the square root scan rate ($\nu^{1/2}$) dependence of the heights and potentials of the peaks are plotted in Fig. 6b and c. It can be recognized that the redox peak currents increased linearly with the scan rate. The correlation coefficient of peak currents, ipc and ipa, was found to be 0.9923 (ipc = 0.0041ν +0.1671) and 0.9921 (ipa = -0.0036ν -0.0433), respectively. This phenomenon suggested that the redox process was an adsorption-controlled process and also the immobilized myoglobin was stable on GCE surface. The results demonstrated that the redox peak currents increased more linearly with the ν in comparison to $\nu^{1/2}$.

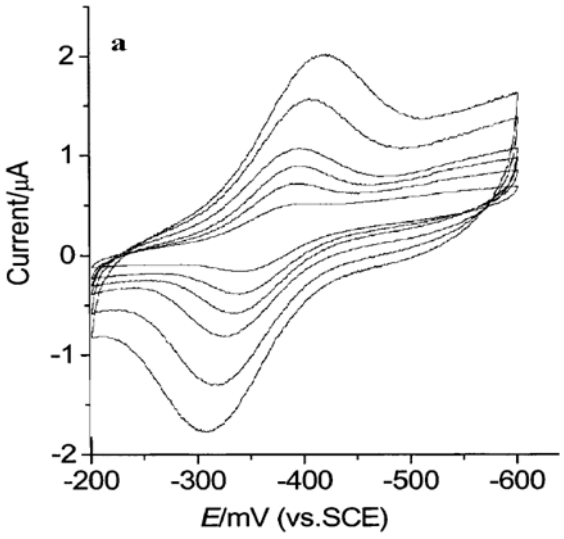

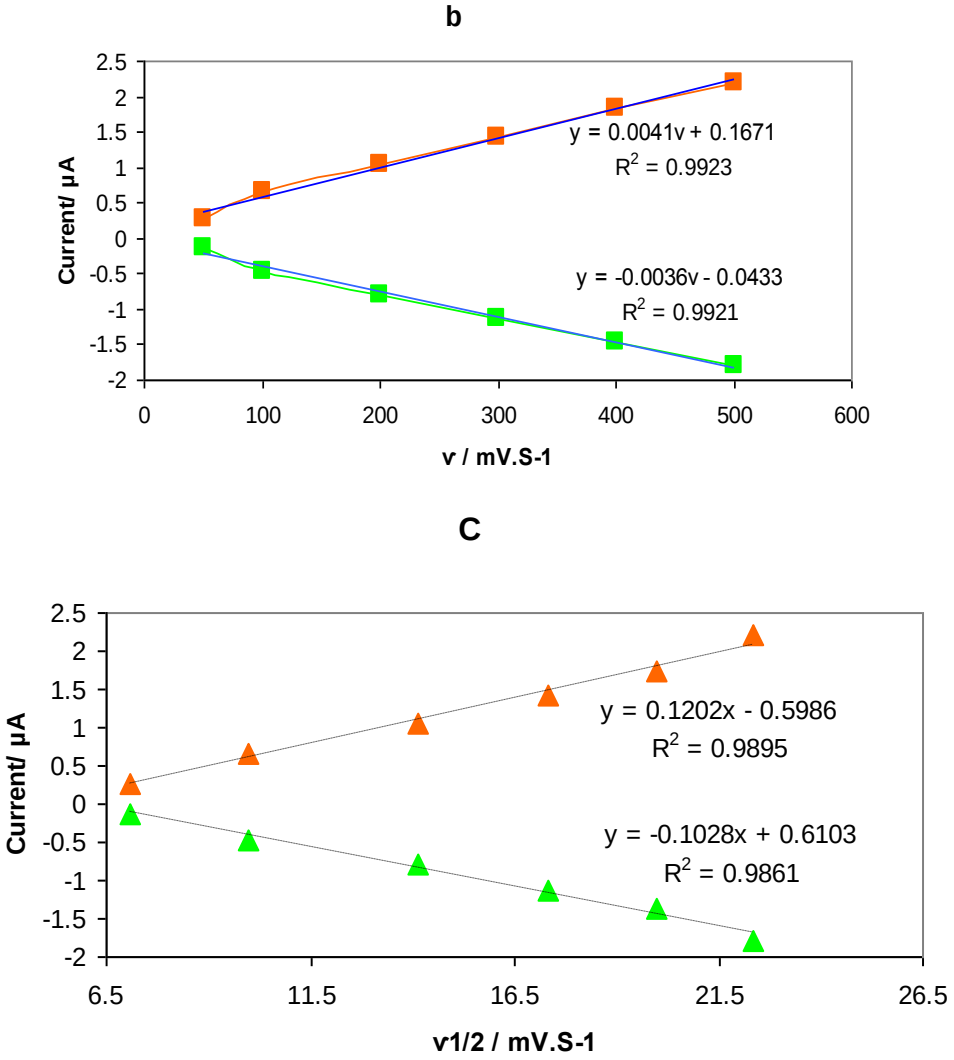


**Figure. 6** (a) CVs of Mb/ CdO Nps/ GCE in PBS 0.1M at different scan rates, from inner to outer; 50, 100, 200, 300,400 and 500 mV $s^{-1}$, the relationship between the peak currents (ipa, ipc) vs., (b) the sweep rates and (c) the square root of sweep rates; red lines are redox peaks and green lines are oxidative peaks.

However, the systematic deviation from linearity is clearly observed in this data, i.e. low scan rates are always observed on one side of the line and the high scan rate points on the other. All these results indicated that the Mb immobilized on CdO Nps/ GCE surface participates in a controlled and quasi-reversible electrochemical process. As the peak-to-peak separation (ΔE) became greater than 200 mV, the apparent heterogeneous electron transfer rate constants (ks) would be easily evaluated based on the Laviron's equations [33]:

$$E_{p,catodic} = E^0 + \frac{RT}{\alpha F} \ln \frac{RTks}{\alpha Fv} \quad (1)$$

$$E_{p,anodic} = E^0 + \frac{RT}{(1-\alpha)F} \ln \frac{RTks}{(1-\alpha)Fv} \quad (2)$$

$$\Delta Ep = Ep_{,\,anodic} - Ep_{,\,catodic} = \frac{RT}{\alpha(1-\alpha)F} \quad (3)$$

$$[\log ks = \alpha \log(1-\alpha) + (1-\alpha)\log\alpha - \log\frac{RT}{nFv} - \frac{\alpha(1-\alpha)nF\Delta EP}{2.3\,RT}] \quad (4)$$

Where α is the electron transfer coefficient and n is the number of transferred electrons at the rate of determining reaction. *R*, *T* and *F* are defined as gas, temperature and Faraday constants, respectively (*R* = 8.314 J $mol^{-1}$ $K^{-1}$, *F* = 96493 C/mol, and *T* = 298 K) and ks is the apparent heterogeneous electron transfer rate constant which can be calculated according to the plot of ΔEp versus ln *v*. The value of ks was estimated to be 2.12 $s^{-1}$, which is slightly larger compared to that of electron transfer of myoglobin on nickel oxide Nanoparticles modified graphite electrode (1.98$s^{-1}$) [8], or electron transfer of myoglobin on zirconia nanoparticles modified carbon paste electrode (0.7 $s^{-1}$) [34]. The ks value directly demonstrated that the electron transfer rate between Mb and glassy carbon electrode in Mb/ CdO Nps/ GCE complex was enhanced.

### *3.5. Design a hydrogen peroxide biosensor by use of reduction peaks of Mb/ CdO Nps/ GCE*

Upon addition of $H_2O_2$ to PBS, the shape of cyclic voltammogram of Mb/ CdO Nps/ GCE for the direct electron transfer of Mb dramatically changed with an increase in reduction current (Fig. 6a), while no obvious change was observed at bare GCE and CdO Nps/ GCE (not shown). The increase in reduction peak current and the decrease in oxidation peak current of Mb at Mb/ CdO Nps/ GCE displayed an obvious electrocatalytic behavior of immobilized Mb towards $H_2O_2$ reduction. Furthermore, the reduction peak current increased with increasing $H_2O_2$ concentration. The electrocatalytic process can be expressed as follows:

$$H_2O_2 + 2MbHFe\ (II) \leftrightarrow 2MbFe\ (III) + 2H_2O \quad (5)$$

In the presence of $H_2O_2$, MbHFe (II) was efficiently converted to its oxidized form, MbFe (III). Subsequently, MbFe (III) was reduced at the electrode surface by direct electron transfer. Increasing $H_2O_2$ concentration led to an enhancement in the current response to Mb Fe (III) reduction as well as an increase in the electrocatalytic current (Fig. 7a). According to Fig. 7b, the calibration range of $H_2O_2$ demonstrates a sensor response.

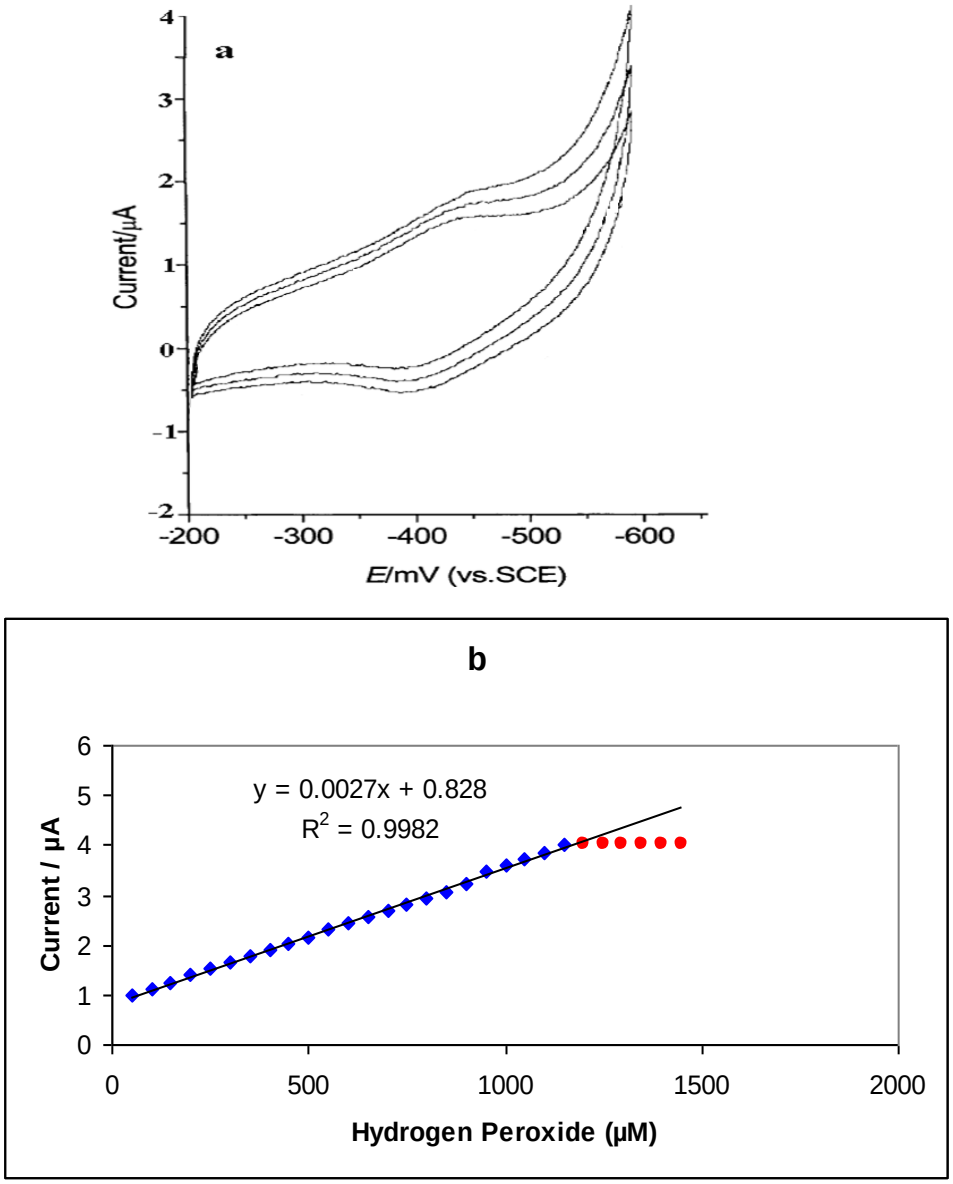


**Figure 7.** (a) Cyclic voltammograms obtained at an Mb/ CdO Nps/ GCE electrode in 0.1M phosphate buffer solution (pH 7.0) for different concentrations of hydrogen peroxide and (b) the relationship between cathodic peak current of Mb and different concentrations of hydrogen peroxide (scan rate: 50 $mVs^{-1}$).

The sensor sensitivity based upon the mean of the slope of the response curve was found to be in the range of 50 to 1150 μM. As can be observed, the sensor response shows a good linearity in this range. The correlation factor ($R^2$) was found as 0.9982. This value is much higher than the our previous results; (15 to 650 μM in research paper: Direct electron transfer of Myoglobin on nickel oxide Nanoparticles modified graphite electrode [8] or 20-100 μM in research paper: Design a Hydrogen Peroxide Biosensor by Cytochrome c and Cadmium Oxide Nanoparticles and its Application in Diagnostic Cancer Cells [34] and 20 to 450 μM in research paper: Direct Electron Transfer of Myoglobin on Zirconia Nanoparticles Modified Carbon Paste Electrode [33].

*3.6. Stability of hydrogen peroxide biosensor*

The stability of Mb/ CdO Nps/ GCE based biosensor has been checked through implementing a series of experiments at the regular intervals of week. It has been found that Mb/ CdO Nps/ GCE based electrochemical biosensor retains its 94% activity after 21 days. The loss of the biosensor activity is not due to the denaturation of myoglobin but it is the result of poor adhesion of cadmium oxide nanoparticles on the glassy carbon electrode. As a result, interface materials do not significantly affect on the operation of biosensor. Undoubtedly, nanotechnology in combination with bioelectrochemistry can extremely influence the development of scientific fields [10-12]. However, a number of challenges remain to be faced particularly the processing of the electrode modifications in a more controlled method. Presenting a great deal of attention, charge transport mechanism in the nano-structured biointerfaces requires further investigation. Worth mentioning, the comprehension of the nanostructured biointerfaces strongly depends on the recent advances in the modern material sciences, including bioelectronics, biocatalysis and biosensing.

## 4. CONCLUSION

The development of nanotechnology, keeping abreast of other sciences, has initiated a great revolution in application of nanoproducts in all scientific fields including electrochemistry and biology. Owing to diverse application of biosensors in industry, the utilization of nanoparticles in the design of biosensors is non-negligible. Our designed biosensor could detect $H_2O_2$ in the range of 50 to 1150 μM, and detection of this amount is very important in medical and industrial works and diagnostic applications.

## References

1. J. J. Lingane, Electroanalytical chemistry, Second ed., *Wiley-Interscience, New York*, 1958.
2. C. Ren, Y. Song, Z. Li, G. Zhu, *Anal. Bioanal. Chem*., 381 (2005) 1179.
3. A. Salimi, E. Sharifi, A. Noorbakhsh, S. Soltanian, *Biophys. Chem*. 125 (2007) 540.
4. D. Britz, *J. Electroanal. Chem*. 88 (1978) 309.
5. C.L. Sanford, B.A. Mantooth, B.T. Jones, *J. Chem. Educ*., 78 (2001) 1221.
6. C.C. Moser, C.C. Page, R. Farid, P.L. *J Bioenerg Biomembr*, 27 (1995) 263.
7. M. Negahdary, M. Torkamani-Noughabi, E. Rezaei, *Advances in Environmental Biology*. 6 (2012) 1095.
8. S. Rezaei-Zarchi, M. Negahdary, *Advances in Environmental Biology*, 5 (2011) 3241.
9. M. Negahdary, C. Mazaheri, S. Rad, M. Hadi, R.Malekzadeh, *International Journal of Analytical Chemistry*, 2012(2012) 1.
10. R. Feynman, There's plenty of room at the bottom. In: *Miniaturization (ed. H.D. Gilbert), New York*, 1961.
11. R. Kurzweil, The Singularity is Near: When humans transcend biology, New York: *Viking Press*, 2005.
12. J.J. Ramsden, Nanotechnology Perceptions, 1 (2005) 3.

13. W. Banzhaf et al., *Nature Reviews Genetics*. 7 (2006) 729.
14. C. Hierold, *J. Micromech. Microengng*. 14 (2004) S1.
15. Jeremy Ramsden, Essentials of Nanotechnology, *Ventus Publishing ApS*. 2009.
16. Farough Salimi, Masoud Negahdary, *Int. J. Electrochem. Sci*., 7 (2012) 7225.
17. F. Scheller, F. Schubert, Biosensors, *Elsevier*, 1992.
18. Xie, X., Subiman, A.A., Guilbault, G.G. and Yang, Z. *Anal.Chim. Acta* 266 (1992) 325.
19. D. P. Hildebrand, H. Tang, Y. Luo, C. L. Hunter, M. Smith, G. D. Brayer, A. G. Mauk, *J. Am. Chem. Soc*. 118 (1996) 12909.
20. Gholamreza Mohseni, Masoud Negahdary, Hossein Faramarzi, *Int. J. Electrochem. Sci*., 7 (2012) 12098.
21. J. F. Rusling, A.-E. F. Nassar, *J. Am. Chem. Soc*. 115 (1993) 11891.
22. A.-E. F. Nassar, J. M. Bobbitt, J. D. Struart, J. F. Rusling, *J. Am. Chem. Soc*. 117 (1995) 10986.
23. Gholamreza Mohseni, Masoud Negahdary, *Int. J. Electrochem. Sci*., 7 (2012) 7033.
24. M. F. Perutz, M. G. Rossmann, A. F. Cullis, H. Muirhead, *Nature*, 185 (1960) 416.
25. M. Brunori and Q. H. Gibson., *EMBO Rep*. 2 (2001) 676.
26. T. Kuo, M.H. Huang, *J. Phys. Chem B*. 110 (2006) 13717.
27. Masoud Negahdary, Seyedeh Anousheh Sadeghi, *Int. J. Electrochem. Sci*., 7 (2012) 6059.
28. V. Drits, J. Środoń and D. D. *Reappraisal of the Kubler Index and the Scherrer Equation Clays and Clay Minerals*. 45 (1997) 461.
29. H. Fan, L. Yang, W. Hua et al., *Nanotechnology*, 15 (2004) 37.
30. Masoud Negahdary, Asadollah Asadi. *Int. J. Electrochem. Sci*., 7 (2012) 5185.
31. D. R. Crow, Principles and applications of electrochemistry, 3rd edn, *Chapman and Hall, London*, 1988.
32. E. Laviron, *J. Electroanal. Chem*., 100 (1979) 263.
33. S. Banapour, M. Mazdapour, Z. Dinpazhooh, F. Salahi, M. Torkamani Noughabi, M. Negahdary, A. Asrari, F. Ghanami, *Advanced Studies in Biology*, 4 (2012) 231.
34. M. Negahdary, S. Rad, M. Torkamani Noughabi, *Advanced Studies in Biology*, 4 (2012) 103.